SUPPLEMENTAL INFORMATION

StarD5: an ER stress protein regulates plasma membrane and intracellular cholesterol homeostasis

Daniel Rodriguez-Agudo[a,b], Leonel Malacrida[c,d], Genta Kakiyama[a,b], Tavis Sparrer[e], Carolina Fortes[a,f], Michael Maceyka[e,g], Mark A. Subler[h], Jolene J. Windle[g,h], Enrico Gratton[c], William M. Pandak[a,b,1], and Gregorio Gil[e,g,1]

[a]Department of Medicine, Virginia Commonwealth University School of Medicine, Richmond, VA, 23298, USA.

[b]McGuire Veterans Affairs Medical Center, Richmond, VA, 23248, USA.

[c]Laboratory for Fluorescence Dynamics, Department of Biomedical Engineering, University of California at Irvine, Irvine, CA, 92697, USA.
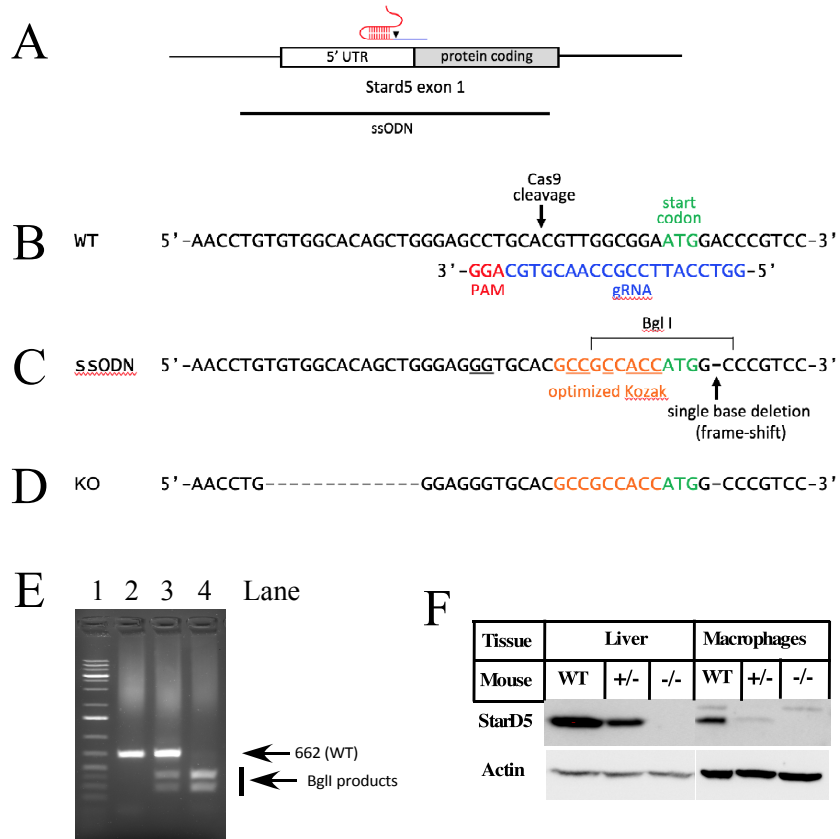
[d]Area de Investigación Respiratoria, Departamento de Fisiopatologia, Hospital de Clinicas, Facultad de Medicina, Universidad de la Republica, Montevideo, Uruguay.

[e]Department Biochemistry and Molecular Biology, Virginia Commonwealth University School of Medicine, Richmond, VA, 23298, USA.

[f]Departmento de Biologia Molecular y Bioquimica, Universidad de Malaga, Spain.

[g]Massey Cancer Center, Virginia Commonwealth University School of Medicine, Richmond, VA, 23298, USA.

[h]Department of Human and Molecular Genetics, Virginia Commonwealth University School of Medicine, Richmond, VA, 23298, USA.

A

5' UTR | protein coding

Stard5 exon 1

ssODN

B WT

Cas9 cleavage

start codon

5'-AACCTGTGTGGCACAGCTGGGAGCCTGCACGTTGGCGGAATGGACCCGTCC-3'

3'-GGACGTGCAACCGCCTTACCTGG-5'

PAM gRNA

C ssODN

Bgl I

5'-AACCTGTGTGGCACAGCTGGGAGGGTGCACGCCGCCACCATGG-CCCGTCC-3'

optimized Kozak

single base deletion (frame-shift)

D KO

5'-AACCTG-----------GGAGGGTGCACGCCGCCACCATGG-CCCGTCC-3'

E

1 2 3 4 Lane

662 (WT)

BgII products

F

Tissue	Liver			Macrophages		
Mouse	WT	+/-	-/-	WT	+/-	-/-
StarD5						
Actin						

Supplemental Figure S1. Generation of StarD5$^{-/-}$ mice using CRISPR/Cas9. (**A-B**) A guide RNA was designed to create a double-strand cleavage 10 bp upstream of the ATG start site. (**C**) Partial sequence of a 200-base repair ssODN, homologous to the StarD5 gene and centered on the Cas9 cleavage site. The ssODN contained a single-base deletion in codon 2 that induces a translational frame-shift, as well as eight mutations (underlined) upstream of the start codon that: (1) create an optimized Kozak sequence for efficient translational initiation, (2) eliminate the Cas9 PAM sequence to prevent retargeting, and (3) create a Bgl I site for screening purposes. (**D**) The sequence changes in StarD5$^{-/-}$ line 3 are shown. (**E**) Pups were screened by PCR followed by Bgl I digestion; *lane 1*, molecular weight markers, *lane 2*, wild type (WT), *lane 3*, heterozygous (+/-), *lane 4*, homozygous (-/-) mouse DNA. (**F**) Total protein extracts were prepared from liver and peritoneal macrophages from wild type (WT), heterozygous (+/-), or homozygous (-/-) mice as indicated and used to perform Western blots for StarD5 and actin as a control.

Fraction	PNS	PM
Lane	1	2
PDI		
Na$^+$/K$^+$ ATPase α-1		

Supplemental Figure S2. Macrophages PM purification. PM was purified from wild type and StarD5$^{-/-}$ macrophages to quantify cholesterol (**Fig. 1**). Aliquots of the post-nuclear supernatant (PNS) and of the PM fraction were used to assess their purity using an ER antibody (anti-protein disulfide isomerase, PDI) and anti-Na$^+$/K$^+$ ATPase α-1 antibodies. A representative preparation is shown.
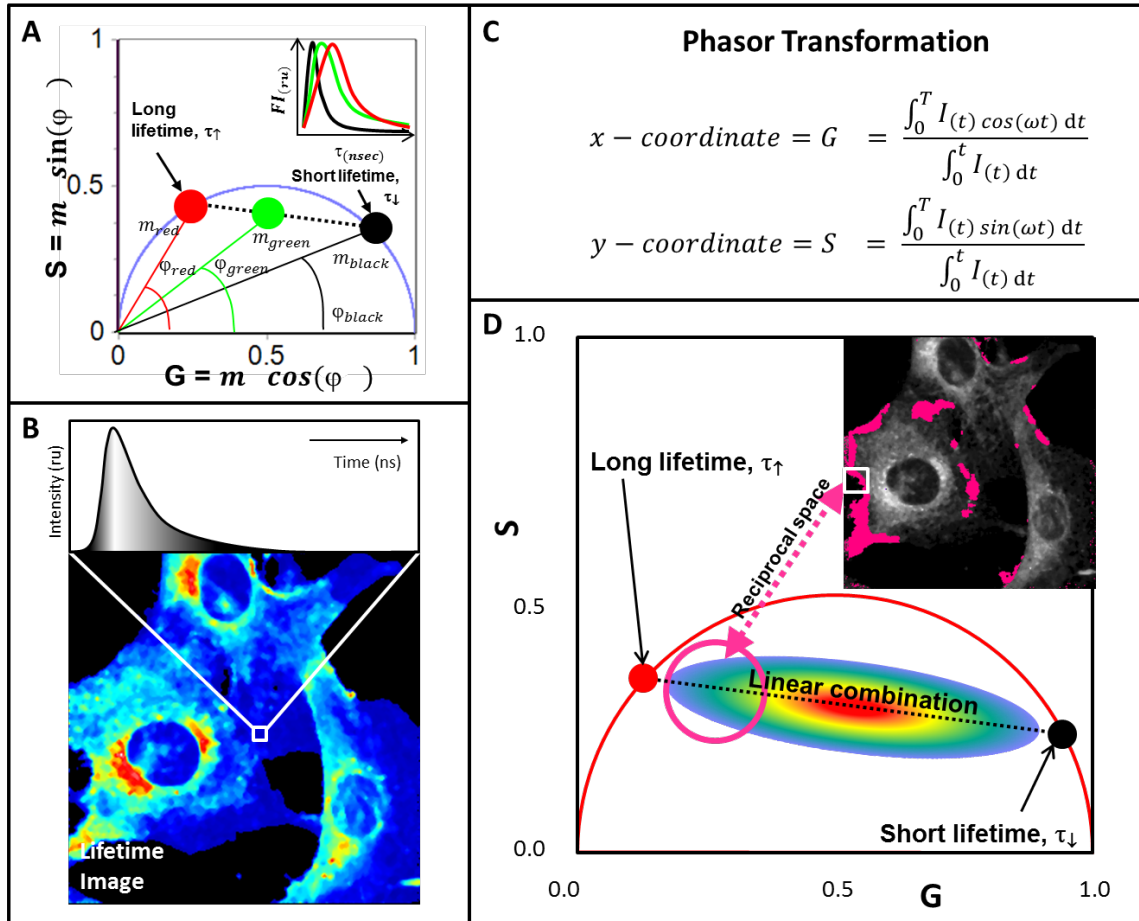
Supplemental Figure S3. Phasor-FLIM analysis and interpretations. (**A**) Simulated phasor plot for long (red dot), short (black dot) and a linear combination of both lifetimes (green dot). At the insert can be identified the simulated decay for the single exponential decay (back and red traces) and the double exponential decay (green trace). Single exponential decays can be found at the universal circle (blue hemi-circle). From coordinate (1,0) to (0,0) the lifetime increases from 0 to ∞. A position inside the universal circle represents at least a linear combination of 2 components. The m and φ represents the modulation and phase for each distribution, respectively. (**B**) Lifetime intensity image for a cell label with LAURDAN. The plot on top illustrates the decay for a single pixel. For every single pixel, the decay is collected and then transformed to the phasor space following the equations in *panel C*. (**C**) Phasor transformation for the lifetime decay at every single pixel. I(t) represents the intensity at given time, ω is the angular modulation frequency (2πf, where *f* is the frequency repetition of the laser) and *T* is the period of the laser. (**D**)

Illustrative phasor plot to show the linear combination and reciprocal properties of phasors. An illustrative distribution of pixels can be observed as an ellipse (in the color scale red mean highest number of pixels in the cluster). Red and black dots represent the extremes of the distribution (long and short lifetimes, respectively). By selecting a region of interest at the phasor plot (pink cursor) it is possible to identify the corresponding pixels at the inset image (reciprocal property).
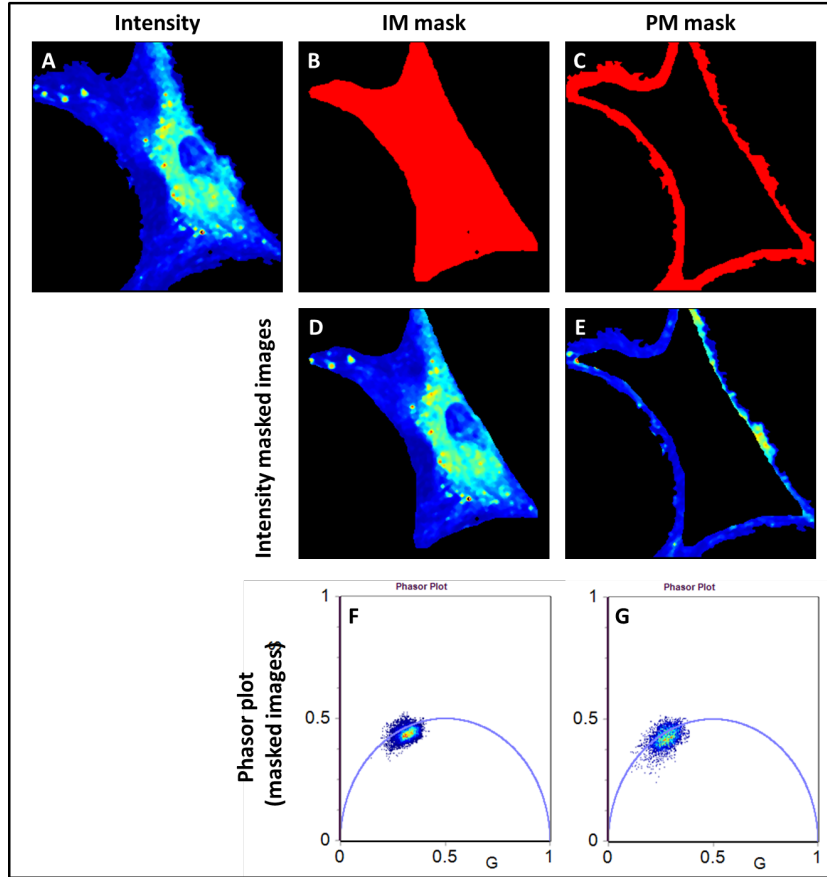
Supplemental Figure S4. Masking procedure for the FLIM data analysis. A) Lifetime intensity image of mouse wild-type macrophage labeled with LAURDAN. (**B and C**) Hand draw masking was performed to separate the information from subcellular regions. Using this procedure two region of interest were independently analyzed, internal and plasma membrane (**B** and **C**, respectively). (**D and E**) FLIM intensity images after application of the masks in **B** and **C**, respectively. (**F and G**) Phasor plots produced by the subcellular regions of interest selected in **D** and **E**, respectively. A full description about using masks can be found in Malacrida *et al* (21).

Supplemental Table S1. Oligonucleotides used in the quantitative qRT-PCR

Oligo	Gene	Gen Bank #	Nucleotides	Sequence
mStarD5-F	m StarD5	NM_023377.4	250-271	CGG GAG AAG TGG GAT GAT AATG
mStarD5-R			354-375	CAC AAA GTC CCT GGG AGA AAT A
mStarD5-P			301-324	ACG GAT ATG CTG TGT GTG AGC AGA
mHMG-CoA reductase-F	m HMG-CoA reductase	BC085083	1893-1915	CTG AAG GGT TTG CAG TGA TAA AG
mHMG-CoA reductase R			1987-2008	CCT GGA CTG GAA ACG GAT ATA G
mHMG-CoA reductase-P			1917-1940	AGG CCT TTG ATA GCA CCA GCA GAT
mNPC1F	mNPC1	NM_008720	1684-1707	CAA GTA GGC GAC GAC TTC TAT ATC
mNPC1R			1764-1783	CGT GGA GCA AAC TCG TAT CA
mNPC1P			643 to 663	ACA CAC TTT CTG TAC TGT GTA CGG GC
mABCA1-F	m ABCA1	NM_013454	126 to 147	GGG TGG TGT TCT TCC TCA TTA C
mABCA1-R			201 to 220	CAC ATC CTC ATC CTC GTC ATT C
mABCA1-P			574 to 594	CCC AGA CCT GTA AAG GCG AAG CTT
mGAPDH-F	m GAPDH	NM_001289726	833-853	GGA GAA ACC TGC CAA GTA TGA
mGAPDH-R			904-922	TCC TCA GTG TAG CCC AAG A
mGAPDH-P			859-882	TCA AGA AGG TGG TGA AGC AGG CAT